We are IntechOpen, the world's leading publisher of Open Access books
Built by scientists, for scientists

6,900
Open access books available

185,000
International authors and editors

200M
Downloads

154
Countries delivered to

Our authors are among the

TOP 1%
most cited scientists

12.2%
Contributors from top 500 universities

CLARIVATE ANALYTICS
BOOK CITATION INDEX
INDEXED

WEB OF SCIENCE™

Selection of our books indexed in the Book Citation Index
in Web of Science™ Core Collection (BKCI)

Interested in publishing with us?
Contact book.department@intechopen.com

Numbers displayed above are based on latest data collected.
For more information visit www.intechopen.com

Chapter

Photoacoustic Imaging for Cancer Diagnosis: A Breast Tumor Example

Reda R. Gharieb

Abstract

Photoacoustic (PA) imaging utilizes laser pulses to deliver energy to an examined object for the generation of ultrasonic waves. Thus, it provides a noninvasive and nonionizing imaging modality. Therefore, it has found clinical use for cancer diagnosis in different organs, e.g., breast, prostate, and thyroid nodules. It offers morphological, functional, and molecular imaging. Moreover, the oxygen saturation in a body can be computed by calculating the wavelength-dependent light absorption coefficients at two different wavelengths. In this chapter, the principle of the PA imaging is introduced for the present book.

Keywords: photoacoustic imaging, backprojection, breast tumor, ARC-shaped ultrasonic detectors

1. Introduction

Photoacoustic (PA) imaging is an emerging diagnostic modality that gets advantage of the optically induced ultrasonic signals in tissues [1–5]. PA imaging in cancer diagnosis relies on the enhanced optical absorption of tumors and the relatively high optical transparency of normal tissues in addition to low acoustic distortion and attenuation of tissues [6]. Cancer cells gradually develop a dense microvascular network, which appears to be a marker that a tumor is aggressively growing and subject to metastasis. Furthermore, not only the amount of blood is substantially higher in malignant tumors compared to normal tissue, but also the blood in malignant tumors tends to be less oxygenated blood than the one in normal tissue. Those abnormalities of blood amount and plus being less oxygenated increase the optical absorption of the cancer tissue in the near-infrared (NIR) region.

PA imaging has been combined with ultrasound imaging and augmented with molecular targeted contrast agents [7, 8]. This makes this hybrid modality capable of imaging cancer at the cellular and molecular level, thus opening diverse opportunities to improve diagnosis of tumors, detect circulating tumor cells, and identify metastatic lymph nodes.

PA imaging consists of shining the object of interest, e.g., prostate/breast by a laser pulse; the light energy absorbed by the object tissues causes a thermal induced mechanical vibration within the tissues. The intensity of the mechanical vibration is

proportional to the light absorption coefficient of different region within the tissues. The mechanical vibration generates ultrasonic waves that propagate outward the object [1, 6, 9]. Theses ultrasonic signals can be recorded at different locations on the object surface and are used to construct an image for the absorption coefficient of the tissue region within the object. This distribution of the light absorption coefficient within the object demonstrates the tumor location and shape. The image construction, which provides an inverse problem solution, can be done analytically or by computed tomography through different backprojection methods [10].

In the next subsections, a review of a PA imaging system is presented. The PA imaging for the breast cancer detection is used as an example. The review highlights the array of the ultrasonic detectors, the received signals, and the formation of the image using a weight and sum backprojection algorithm.

2. General PA imaging system

Figure 1 shows a block diagram of the photoacoustic imaging principle. As shown, laser pulse is used to deliver optical energy to an absorptive object, e.g., breast/prostate tissues, whole body of a small animal. The tissues absorb some energy from the laser light and get heated up. After heating, the tissues expand or vibrate in order to release the absorbed heat energy. This sudden and fast expansion of tissues in turn causes sound waves to be generated and they are in the frequency range of Mega Hertz (Ultrasound). These ultrasonic waves are recorded using a set of piezoelectric detectors. The time taken to receive ultrasound after the laser pulse has been given is used to find the location of the tissues which vibrate. Thus, the ultrasonic signals can be handled so that to provide a morphological image in two- or three-dimensional for the absorptive object. The image formation is accomplished utilizing different backprojection methods [10]. These methods take into account the light distribution, the geometry of the ultrasonic detectors array, and the directivity pattern of each detector. In [11], the recent advancement of light-emitting diode (LED) technology has shown to provide a less expensive and more safety source of light to replace the class-IV laser systems. Recently, integrating a microrobotic system and PA imaging has enabled deep imaging and precise control of the micromotors in vivo [12].

Near-infrared (NIR) light (wavelength range of 700–2500 nanometers) is used as a laser pulse to deliver energy to the tissues. This is because of the fact that NIR can penetrate skin since the skin absorbs very less light at longer wavelengths. However, as NIR skips past the skin to deeper tissues, water and other components in deeper tissues absorb NIR and therefore get heated up and release the ultrasonic waves.
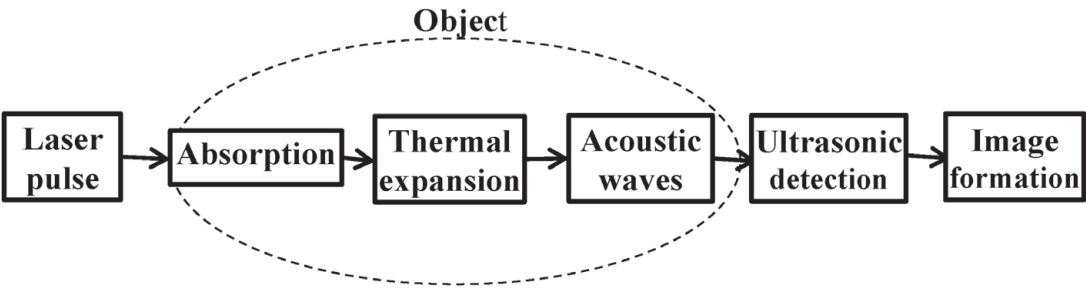
Figure 1.
A general block diagram of PA imaging principle.

3. Advantages and disadvantages of PA imaging

Advantages include:

1. nonionizing imaging since it relies on just NIR light (optical radiation) and ultrasound;

2. high contrast and good spatial resolution. The high contrast is due to the use of the optical contrast absorption and the good spatial resolution is due to the use of ultrasonic signals resolution. Thus, it is a single hybrid imaging modality;

3. provides better depth of penetration than different optical imaging and better spatial resolution than ultrasonic imaging; and

4. nanoparticles can be used to enhance the tissue heating process and therefore the ultrasonic signals and the final image.

Disadvantages include:

1. depth of penetration and distribution of light are issues.

4. Ultrasound signals and backprojection

As illustrated by **Figure 2**, the ultrasonic pressure wave received at a circle of radius r_0 in the 2D space due to a laser pulse is given by [13]

$$p(r_0, t, \varphi) = \frac{v_s B I_0}{4\pi C} \frac{\partial}{\partial t} \oint_{|r_0 - r| = v_s t} \frac{A(r)}{|r_0 - r|} dr \quad (1)$$

where v_s is the speed of the acoustic waves; B is the coefficient of volumetric thermal expansion; C is the specific heat capacity; I_0 is a scaling factor proportional to the incident radiation intensity; and $A(r)$ describes the to-be-reconstructed electromagnetic absorption property of the medium at r, given $p(r_0, t)$.
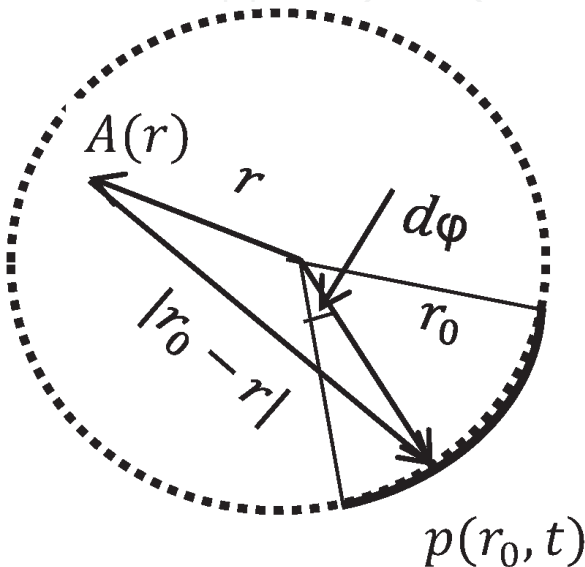
Figure 2.
The acoustic pressure wave $p(r_0, t)$ detected on an ARC of radius r_0 and angle φ due to the electromagnetic absorption $A(r)$.

For 2D image formation using the recorded acoustic pressure $p(r_0, t)$, the approximate inverse solution is given by [14]

$$A(r) = -\frac{r_0^2 C}{4\pi B I_0 v_s^4} \int_\varphi \frac{1}{t} \frac{\partial p(r_0, t)}{\partial t}\bigg|_{t=|r_0-r|/v_s} d\varphi \qquad (2)$$

This implies that first, compute time-derivative of the pressure wave, divide the resultant by t, and finally, integrate over the ARC angle. Notice that r is determined by the time the wave taken to travel from the point r to r_0.

Thus, practically to detect the ultrasonic signals released form the absorptive object excited by the laser pulse, a set of the piezoelectric sensors are used. These sensors are arranged in an array of a certain geometry either linear, surface, curvature, etc. The number of sensors, the geometry of the array, and the directivity of each sensor, the ability of the sensor to receive a signal from only a certain direction, are important factors for the image quality. Each sensor is followed by a low-noise amplifier to amplify the detected signal. **Figure 3** shows the geometry of an ARC-shaped array of 64 sensors that has been adopted for breast cancer imaging [6]. These sensors are uniformly distributed on an angle of 166°. All the sensors have the directivity, the maximum gain, to the center of the ARC, the point $(0, 0)$. Thus, the recorded signal by the kth sensor in time-domain can be expressed by
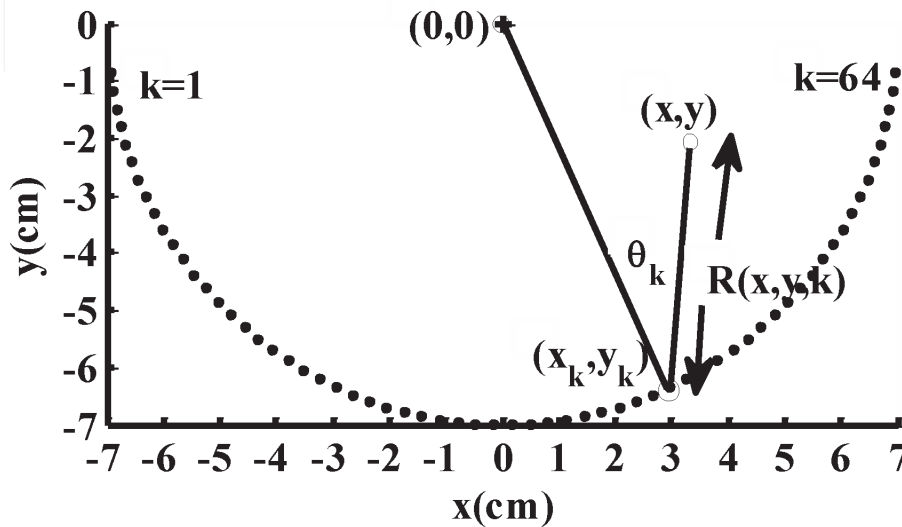
$$v_k(t), t = 0, T, 2T, 3T, \dots \qquad (3)$$

where T is the sampling time.

Assuming uniform light distribution within the tissue, the back projection of the kth sensor signal is given by

$$G_k(x, y) = \overline{v_k}\left(\frac{R\big(x - x_k, y - y_k\big)}{v_s}\right) R\big(x - x_k, y - y_k\big) \cos(\theta_k(x, y)), \quad -7 < x < 7,$$

$$-4 < y < 0$$

$$(4)$$

where $\overline{v_k}$ is the velocity potential computed by the time-integration of the received pressure signals; and $v_s = 1540$ m/ sec is the speed of sound in tissues.
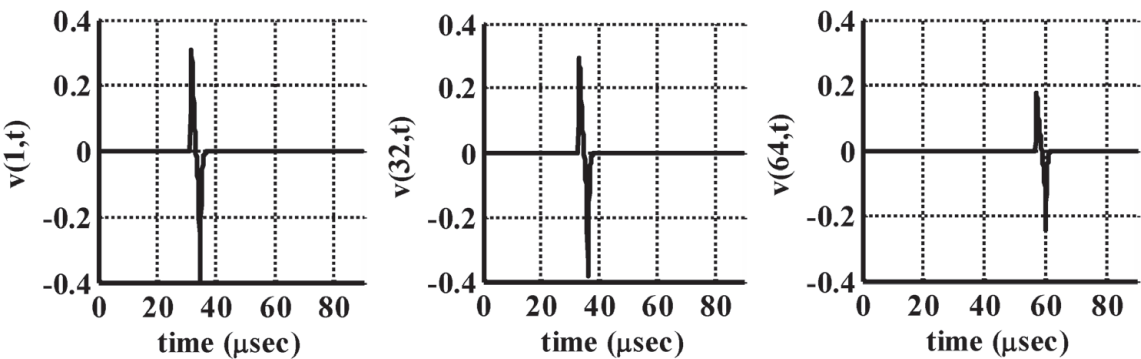

Figure 3.
ARC-shaped PA ultrasonic detecting array.

We can also restrict the projected location (x,y) for only $\{(x,y) : |\theta_k(x,y)| \leq \frac{\pi}{2}\}$. For the M sensors, the back projection is done by the summation of (4) over the M sensors, that is

$$G(x,y) = \sum_{k=1}^{M} G_k(x,y) \tag{5}$$

5. PA signal and image processing

In PA imaging, ultrasonic signals are received in noise; thus, small objects become buried in noise. Hence, prior to image formulation, different signal processing techniques can be used to remove the noise, enhancing the signal-to-noise ratio. Filtering in addition to principal component analysis (PCA) are widely used techniques [15–24]. Also, multiresolution analysis, utilizing wavelet analysis and subband decomposition, of PA signals can be used to obtain images at different scales [17, 20–24]. Furthermore, post-image formulation; image processing methods can be used to enhance the visualization of the image. These methods include contrast enhancement, edge detection, segmentation, and pattern

Figure 4.
Signals received at sensors number 1 (most top-left side), 32 and 64 (most top-right side) in the system geometry of **Figure 3**. *The simulated tumor is a uniform circular disk of radius 0.25 cm centered at $(-2, -2)$. The set of the signals are used for the construction of the image in* **Figure 5**.
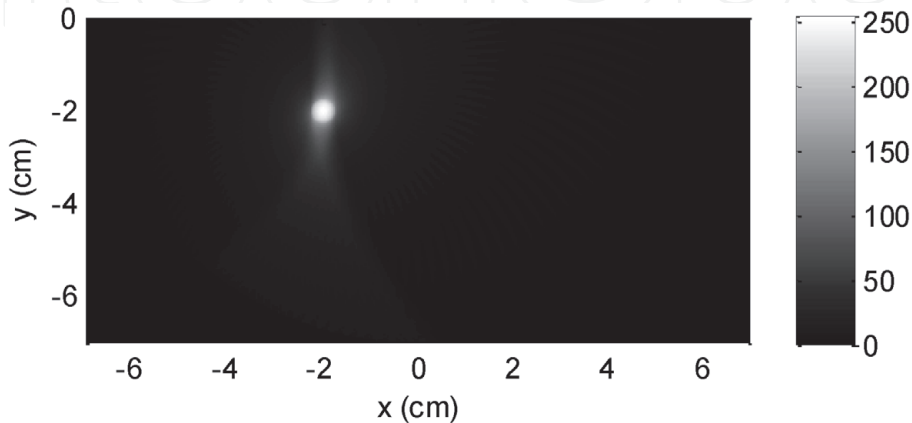
Figure 5.
Image formation by the back projection algorithm in (4) and (5). It is obvious that the tumor is extracted. Notice that the problem here is simplified, no noise is assumed, the light distribution is assumed uniform within the overall examined object, which is not practically a simple task.

recognition [4]. Deep learning is expected to play a good role in extracting more features PA imaging. In [25], deep learning is used to construct PA image from sparse data (**Figure 4**).

6. Conclusion

Simply saying, PA imaging utilizes the ultrasonic signal sent by the examined object to formulate an image for the distribution of the NIR light absorption coefficient within this object. This distribution differentiates abnormal tissues (malignant) from the normal one. Utilizing the absorption coefficients due to two different wavelengths provides information about the oxygen saturation. Hybrid modalities by combing PA image and pure ultrasound image offer imaging at cellular and molecular level. The challenges associated with the PA imaging modality are to deliver the examined object with a uniform distributed light independent of the depth and shape of this object and to reconstruct an online three-dimensional image for image-guided biomedical applications.

Author details

Reda R. Gharieb
Faculty of Engineering, Assiut University, Egypt

*Address all correspondence to: rrgharieb@gmail.com

IntechOpen

References

[1] Oraevsky AA, Jacques SL, Tittel FK. Determination of tissue optical properties by piezoelectric detection of laser-induced stress waves. In: Proceedings of SPIE (The Society of Photo-Optical Instrumentation Engineers). Photons Plus Ultrasound: Imaging and Sensing, Vol. 1882, January 1993. 1993. pp. 86-101

[2] Shi J et al. High-resolution high-contrast mid-infrared imaging of fresh biological samples with ultraviolet-localized photoacoustic microscopy. Nature Photonics. 2019;**13**(9):609-615

[3] Lin L, Wang LV. Single-breath-hold photoacoustic computed tomography of the breast. Nature Communications. 2018;**9**(2352):1-9

[4] Wang B, Su JL, Amirian J, Litovsky SH, Smalling R, Emelianov S. Detection of lipid in atherosclerotic vessels using ultrasound-guided spectroscopic intravascular photoacoustic imaging. Optics Express. 2010;**18**(5):4889-4897

[5] Mallidi S, Luke GP, Emelianov S. Photoacoustic imaging in cancer detection, diagnosis, and treatment guidance. Trends in Biotechnology. 2011;**29**(5):213-221

[6] Ermilov S et al. Detection and noninvasive diagnostics of breast cancer with 2-color laser optoacoustic imaging system. In: Proceedings of SPIE. Photons Plus Ultrasound: Imaging and Sensing, Vol. 6437. 2007. pp. 1-11

[7] Mehrmohammadi M, Yoon SJ, Yeager D, Emelianov SY. Photoacoustic imaging for cancer detection and staging. Current Molecular Imaging. 2013;**2**(1):89-105

[8] Yaseen MA, et al. Hybrid optoacoustic and ultrasonic imaging system for detection of prostate malignancies. In: Proceedings of SPIE.

Photons Plus Ultrasound: Imaging and Sensing. 2008

[9] Wang LV. Tutorial on photoacoustic microscopy and computed tomography. IEEE Journal of Selected Topics in Quantum Electronics. 2008;**14**(1):171-179

[10] Anastasio MA. Advancements in image reconstruction for photoacoustic computed tomography. In: Proceedings of SPIE. Photons Plus Ultrasound: Imaging and Sensing, Vol. 108780, March 2019. 2019

[11] Hariri A et al. The characterization of an economic and portable LED-based photoacoustic system to facilitate molecular imaging. Photoacoustics. 2018;**9**:10-20

[12] Wu Z et al. A microrobotic system guided by photoacoustic computed tomography for targeted navigation in intestines in vivo. Science robotics. 2019;**4**(32):1-11

[13] Xu Y, Wang LV, Ambartsoumian G, Kuchment P. Reconstructions in limited-view thermoacoustic tomography. Medical Physics. 2004;**31**(4):724-733

[14] Xu M, Wang LV. Universal back-projection algorithm for photoacoustic computed tomography. Physical Review E. 2005;**71**(1):016706-1:7

[15] Wang Y, Xing D, Zeng Y, Chen Q. Photoacoustic imaging with deconvolution algorithm. Physics in Medicine and Biology. 2004;**49**:3117-3124

[16] Manohar S, Dantuma M. Current and future trends in photoacoustic breast imaging. Photoacoustics. 2019;**16**(100134):1-27

[17] Zeng L, Xing D, Gu H, Yang D, Yang S, Xiang L. High antinoise photoacoustic tomography based on a

modified filtered backprojection algorithm with combination wavelet. Medical Physics. 2007;**34**(2):556-563

[18] Li PC, Wei CW, Sheu YL. Subband photoacoustic imaging for contrast improvement. Optics Express. 2008; **16**(25):20215-20226

[19] Gao F, Feng X, Zhang R, Liu S, Zheng Y. Adaptive photoacoustic sensing using matched filter. IEEE Sensors Letters. 2017;**1**(5):1-3

[20] Holan SH, Viator JA. Automated wavelet denoising of photoacoustic signals for circulating melanoma cell detection and burn image reconstruction. Physics in Medicine and Biology. 2008;**53**:N227-N236

[21] Zalev J, Kolios MC. Detecting abnormal vasculature from photoacoustic signals using wavelet-packet features. In: Proceedings of SPIE. Photons Plus Ultrasound: Imaging and Sensing, Vol. 7899. 2011. p. 78992M-1:15

[22] Zhou M, Xia H, Lan H, Duan T, Zhong H, Gao F. Wavelet de-noising method with adaptive threshold selection for photoacoustic tomography. In: Proceedings of the Annual International Conference of the IEEE Engineering in Medicine and Biology Society, July 2018. 2018. pp. 4796-4799

[23] Zhou M et al. A noise reduction method for photoacoustic imaging in vivo based on EMD and conditional mutual information. IEEE Photonics Journal. 2019;**11**(1):1-10

[24] Frikel J, Haltmeier M. Efficient regularization with wavelet sparsity constraints in photoacoustic tomography. Inverse Problems. 2018; **34**(2):1-28

[25] Antholzer S, Haltmeier M, Schwab J. Deep learning for photoacoustic tomography from sparse data. Inverse Problems in Science and Engineering. 2019;**27**(7):987-1005